DISCUSSION AND SIMULATION ABOUT THE EVALUATION OF THE EMITTER SERIES RESISTANCE

Gabriel Micard, Giso Hahn

University of Konstanz, Department of Physics, 78457 Konstanz, Germany

Author for correspondence: gabriel.micard@uni-konstanz.de, Tel.: +49 7531 88 2060, Fax: +49 7531 88 3895

ABSTRACT: The emitter series resistances ($R_{s,emi}$) can be extracted from experimentally measured JV curves using the two-light intensity method (TLIM) but it can also be calculated from the emitter geometry using analytical formulas and finally also computed with arbitrary precision using finite element simulation (FES). On the one hand formulas and FES consider $R_{s,emi}$ as distributed, on the other hand the TLIM assumes $R_{s,emi}$ not to be distributed. The derivation of formulas for a lumped $R_{s,emi}$ assumes a spatially uniform current density source, which is the case in short circuit condition (J_{sc}), less at maximum power point (mpp) and is wrong at open circuit. We compare at mpp the results of TLIM, analytical formulas and FES for which the current density source is a 1D simulated JV curve. In the case of a low/high sheet resistance homogeneous emitter, but also for a selective emitter, these methods agree well and the impact on cell efficiency is particularly small. This is partially explained by the fact that the voltage drop and so the spatial distribution of the current density source over the emitter is small at mpp. We also clarify many issues about the various methods used and discuss the limitation of not taking into account Joule losses induced by diffusion.

Keywords: Emitter, Series resistance, Joule loss, Modeling

1 INTRODUCTION

In silicon solar cells, the series resistance is an important and intricate parameter that has to be minimized in order to reduce fill factor losses and thus cell efficiency losses. The series resistance appears as a single resistance in series in the two-diode model in which, neglecting the parallel resistance, it describes alone all the Joule losses present in a solar cell.

The series resistance as defined by the two-diode model, however, supposes that there is a unique potential to bias the diode which is, strictly speaking, not correct because of the distributed character of the series resistance.

Speaking more specifically of the series resistance contribution of the emitter $R_{s,emi}$, the potential distribution over the emitter surface is usually said to have a negligible consequence on the final current density voltage (JV) characteristics, because this potential distribution is usually small for not too high emitter sheet resistance. One should, however, note that the tendency is to use higher emitter sheet resistances to get a better blue response which could hinder this assumption.

Using the fact that the series resistance should dissipate the same amount of Joule heat than the solar cell, one can make a calculation of the series resistance from the sheet resistance and the front grid geometry, assuming implicitly that the distributed current density source is homogeneously constant. The series resistance derived this way is independent of the current density delivered by the solar cell.

One should, however, remark that the assumption of a homogeneously constant current density source is essentially correct around short circuit (J_{sc}) conditions, but slightly erroneous around the maximum power point (mpp) and completely wrong around open circuit (V_{oc}) conditions because of an increasing curvature of the JV curve at the two aforementioned points. This implies that the series resistance becomes a function of the inhomogeneity of the current density source distribution and thus a function of the cell's bias.

From the experimental side, determining the series resistance is performed at best by the two-light intensity method (TLIM), which is known to be very accurate while not assuming any particular structure of the diode network of the solar cell. This method also relies on the assumption of a lumped series resistance and is not tight to Joule heat power dissipation consideration.

The question raised by this article is therefore how these different ways of determining the series resistance agree with each other knowing that they all use different assumptions which seem difficult to reconcile and to assess the validity.

Using the definition of the series resistance in terms of equivalent Joule loss dissipation, we compare the exact calculation of the series resistance by finite element simulation (FES) to its calculation from the sheet resistance and geometry as well as its estimation by TLIM in order to understand and comment on the various observed discrepancies.

2 THEORY AND METHODS

2.1 FlexPDE simulation

The solar cell is modelled by a distributed junction, which delivers current into the resistive sheet of the emitter with the current being collected at the finger and busbar located at the edge of the emitter sheet.

In a thin layer of sheet resistance R_{sh} in which the current density is supplied by a current density source that could be voltage dependant $J_{source}(V)$, the partial differential equation (PDE) to be solved for the potential distribution is of the Poisson form:

$$\nabla\left((1/R_{sh})\cdot\nabla V\right) = -J_{source}(V) \qquad (1)$$

In the present case $J_{source}(V)$ is the JV curve obtained from a PC1D simulation discarding the series resistance.

The numerical solving of Eq. 1 is performed numerically using the finite element solver FlexPDE [1] on a rectangular area ranging from the finger edge to the center point between two fingers in x and from the busbar edge to the center point between two busbars. The finger and busbar edges are maintained at a constant potential V_0 (the external potential of the cell) that is varied during the simulation while the two other edges are symmetry boundaries in which no carrier flow occurs implying $\nabla V = 0$.
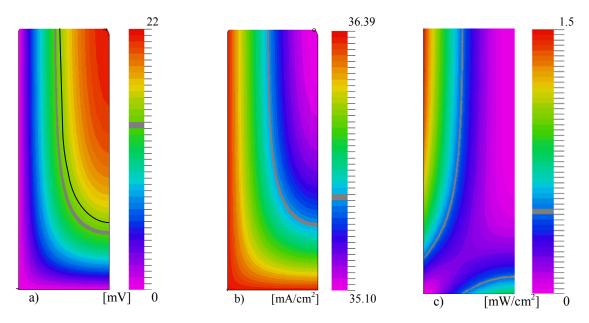
22 36.39 1.5

a) [mV] 0   b) [mA/cm^2] 35.10   c) [mW/cm^2] 0

Figure 1: Distribution of a) the potential drop, b) the current density source distribution, and c) the dissipated power density in the emitter at the busbar (left edge) and finger (bottom edge) corner for an inter-finger distance of 1.9 mm, an inter-busbar distance of 50 mm and an emitter sheet resistance of 130 Ω/□ (zoom on busbar/finger corner). The grey level indicates the average current density source value J_{avg} in b), the average power loss density in c), and with $R_{s,emi} \cdot J_{avg}$ the potential drop of the lumped series resistance crossed by J_{avg} in a). The black line in a) indicates the location of the average current density of b) in the potential map of a).

Varying the finger/busbar potential V_0 is therefore equivalent to varying the cell bias for which the current density of the cell could be obtained by averaging J_{source} over the whole domain. This way one obtains a JV curve of the full solar cell from this simulation. The potential drop distribution over the emitter is therefore $V(x,y)-V_0$ and is represented in Fig. 1a at $V_0=V_{mpp}$. While this potential drop is small (22 mV max) it is sufficient to induce an inhomogeneous current density distribution (difference of 1 mA/cm^2 max) as one can see in Fig. 1b. Finally, the dissipated power density distribution in the emitter can be calculated using Eq. 2 as displayed in Fig. 1c.

$$\Phi_{dis} = |\nabla V|^2 / R_{sh} \qquad (2)$$

$$R_{s,emi} = A. \int_A \Phi_{dis} dS / \left(\int_A J_{source}(V) dS \right)^2 \qquad (3)$$

where A is the area of the simulated domain. Details about the theory are available in [2].

2.2 Two Light Intensity Method (TLIM)

In order to extract the series resistance from experimental JV curves we use the TLIM from Wolf and Rauschenbach [3].

One measures JV curves at various light intensity and assumes firstly that modifying the illumination just translates the JV curve in the J axis by an amount ΔJ. But because of the presence of the series resistance the V axis should also be translated by an amount $\Delta V = R_s. \Delta J$.
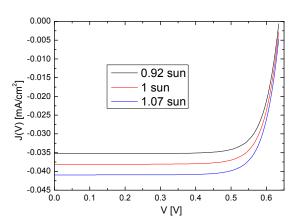

Figure 2: JV curves simulated at 0.92, 1 and 1.07 sun.

Knowing the total power dissipated by Joule effect as well as the average current density crossing the structure one can compute the emitter series resistance as
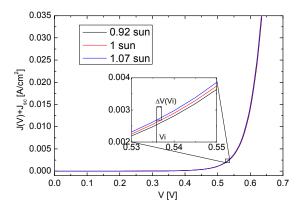

Figure 3: JV curves simulated at 0.92, 1 and 1.07 sun shifted up by their respective J_{sc}.

One must first note that this method assumes the linearity of the solar cell response to the illumination level. This is strictly speaking not true because of the

nonlinear behavior of the recombination mechanisms to the injection and so to the illumination level. However, if one chooses a small difference of illumination, the linearity can be assumed. Therefore we chose 0.92, 1 and 1.07 sun delivering JV curves like shown in Fig. 2.

While ΔJ can be taken by the difference of J_{sc} of the two curves and is assumed to be constant for the whole curve, one can consider that the ΔV is not constant and depends on the voltage.

For this one makes the first translation by ΔJ and evaluates the ΔV for various voltages V_i like shown in Fig. 3. This modification of the TLIM to get an $R_s(V)$ curve was suggested by Swanson [4].

In order to increase the accuracy of the R_s determination the linear relationship $\Delta V = R_s \cdot \Delta J$ is evaluated at 0.92/1 sun and 1/1.07 sun and R_s is fitted according to a least square criteria.

2.3 Geometry based emitter series resistance formula

In the case of a spatially uniform source current density distribution N. C. Wyeth [5] showed that the series resistance of the emitter could be calculated as

$$R_{s,emi} = \frac{1}{12} R_{sh} a^2 \left[1 - \frac{a}{b} \frac{96}{\pi^5} \sum_{m=0}^{\infty} (2m+1)^{-5} \tanh \left\{ (2m+1)\pi \frac{b}{a} \right\} \right] (4)$$

where a is the interfinger distance and b the interbusbar distance. While this result is an infinite series the fact that its leading term has a -5 power makes it very fast converging. Then, five terms are enough to get an accuracy higher than 6 digits for the series resistance.

2.4 PC1D simulations

A standard solar cell with a bulk of thickness t=200 μm, resistivity ρ=2 Ωcm, a bulk lifetime τ=500 μs and an emitter of 77 Ω/□ is simulated by PC1D [6] at 0.92, 1 and 1.07 sun while discarding any external resistance.

A simulation of the same structure but 'cutting' the emitter profile (simulating an etching of the front surface [7]) so that its sheet resistance becomes 130 Ω/□ and considering the difference of front surface recombination velocity due to the lower surface dopant concentration is performed at 0.92, 1 and 1.07 sun.

These JV curves are assumed to include only the bulk contribution to the series resistance.
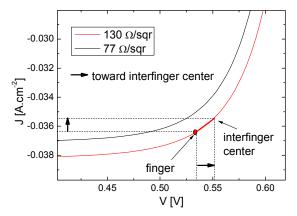

Figure 4: JV curves around mpp obtained at 1 sun for the emitters of R_{sheet}=77 and 130 Ω/□ without additional series resistance contribution.

One can see in Fig. 4 that the source current density distribution observed in Fig. 1b is simply a consequence of the potential distribution shown in Fig. 1a.

2.4 Series resistance of the bulk

The TLIM applied to the final JV curve delivers the total series resistance of the solar cell. Therefore we have to subtract the contribution of the bulk to get only the contribution of the emitter.

The estimation of the series resistance of the bulk $R_{s,bulk}$ can be performed analytically by using the formula $R_{s,bulk}=\rho \cdot t$ [8] with thickness t making in our case $R_{s,bulk}$=0.04 Ωcm^2.

One could also estimate $R_{s,bulk}$ using the TLIM on the PC1D curves. The comparison of the $R_{s,bulk}$ estimations for both emitters and analythical is shown in Fig. 5.

One observes first that the values extracted by TLIM are very much voltage dependent and that estimations for high and low sheet resistance emitters are almost the same as one should expect, because the bulk is the same for both simulations. The calculated value overestimates the extracted series resistance for high voltage while it underestimates it for low voltage.

The sharp increase of $R_{s,bulk}$ at low voltage is probably an artifact due to the fact that the TLIM is far less precise in this voltage range because ΔV becomes large and the relative error on the corrected JV curve interpolation becomes large (see Fig. 3).
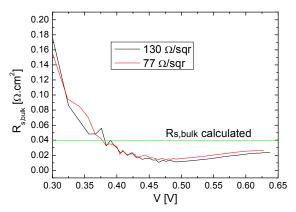

Figure 5: Extracted series resistance of the bulk using the TLIM in comparison with the calculated value from the geometry.

The underestimation of $R_{s,bulk}$ at high voltage could be attributed to the fact that the diffusion is important in the bulk and the series resistance the way it is defined implies only drift.

To be more precise one can say that physically the Joule heat is caused by interactions between the electrons that form the current density and the atomic ions that make up the body of the conductor. These electrons are usually assumed to be accelerated by an electric field (drift) in which case the Ohm law applies at equilibrium.

This definition is hindered in the case of crystalline silicon solar cells because carrier diffusion is the dominant transport mechanism in the bulk and therefore generates Joule heat independently and without drift. A more general formulation of the Joule loss in cases where one should also consider diffusion has been developed by Brendel et al. [9]. This is, however, not the purpose of this article.

The $R_{s,bulk}$ curves extracted from the PC1D simulation are therefore doubtful in many respect and we will use them with caution in the following in this article.

3 STUDY OF HOMOGENEOUS EMITTERS

3.1 Low sheet resistance emitter

Studying the case of the homogeneous emitter with R_{sh}=77 $\Omega/\square$ we first compare the series resistance extracted by FlexPDE at 0.92 sun and at 1.07 sun to see the largest variations possible due to the cell injection non linearity.

The two $R_{s,emi}$ values are identical for short circuit condition and as long as we are in the plateau of the JV curves. This value corresponds exactly to the value computed for this problem by the analytical formula developed by Wyeth [5] from geometrical consideration and sheet resistance only that is shown in purple in Fig. 6.
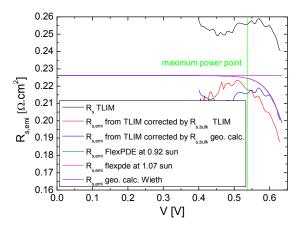

Figure 6: Comparison of $R_{s,emi}$ for: TLIM extracted values (black) corrected by $R_{s,bulk}$ obtained by TLIM (red) or calculated from the geometry (blue), $R_{s,emi}$ value computed by FlexPDE at 0.92 and 1.07 sun illumination (dark green and pink curve, respectively), and $R_{s,emi}$ computed from the geometry by Wyeth's formula (purple) for the 77 $\Omega/\square$ homogeneous emitter.
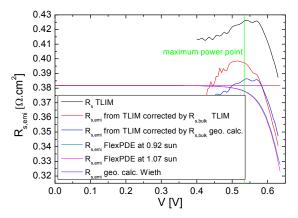

Figure 7: Comparison of $R_{s,emi}$ for: TLIM extracted values (black) corrected by $R_{s,bulk}$ obtained by TLIM (red) or calculated value from the geometry (blue), $R_{s,emi}$ computed by FlexPDE at 0.92 and 1.07 sun illumination (green and pink curve, respectively) and the $R_{s,emi}$ computed from the geometry by Wieth's formula (purple) for the homogeneous emitter with $R_{sh,emi}$=130 $\Omega/\square$

One, however, observes a decay of the R_s value at high voltage corresponding to the inhomogeneous distribution of the current density source as one can see in Fig. 1b. We explain this decay as a consequence of the fact that the maximum source current density is obtained close to the finger/busbars and thus this higher power delivered suffers less Joule losses because of the reduced path of the current to the finger/busbar. Therefore, the equivalent series resistance decays. A very slight difference is then observed in the decaying phase of $R_{s,emi}$ between the two-illumination JV curves. This difference is, however, so small that it can be neglected.

Now applying the TLIM to the JV curves simulated by FlexPDE delivers a R_s value that systematically overestimates the FlexPDE values (black curve in Fig. 6). If, however, one subtracts $R_{s,bulk}$ obtained from the TLIM applied to the PC1D curves, the value is in much better agreement, slightly underestimating it for the 77 $\Omega/\square$ emitter (red curve in Fig. 6).

One can observe that the decay of R_s is also observed for the TLIM extracted values. However, the $R_{s,emi}$ decay at low voltage does not correspond to the trend of the FlexPDE curve and is a consequence of the sharp increase of $R_{s,bulk}$ observed in Fig. 5. As this increase was already doubted due to the low accuracy of the TLIM method in this voltage range, it seems also relevant to correct the $R_s(V)$ curve by the geometrically calculated value of $R_{s,bulk}$ (blue curve in Fig. 6). This new correction is not obviously better than the previous one except at high voltage where the match is almost perfect.

The discrepancy at mpp is nevertheless only of the order of 0.01 $\Omega.cm^2$ which remains pretty low. And therefore one can state that the methods agree with high accuracy.

3.2 High sheet resistance emitter

The discrepancy observed in Fig. 7 between the two FlexPDE JV curves obtained at 0.92 and 1.07 sun is more significant than with the low sheet resistance emitter but still remains very low and can therefore be neglected. When corrected by the series resistance of the bulk (geometrically calculated), the series resistance obtained by TLIM is very good matching the one calculated by FlexPDE around mpp, but this time slightly overestimating, contrary to the case of the low R_{sh} emitter for an unclear reason. Correcting by the TLIM extracted $R_{s,bulk}$ the discrepancy is higher.

Like for the low R_{sh} emitter, the discrepancy is low even if R_{sh} was significantly increased.

3.3 Effects on the PV curves

Up to now it was checked that various methods to determine the series resistance agree quite good between each other. However, the effect of considering the series resistance lumped or distributed concerning the efficiency remains to be investigated at mpp.

For this purpose we compare the JV curve obtained by FlexPDE and the one obtained from PC1D while including the influence of a lumped series resistance as determined by geometry based formulas (corresponding also to the one obtained by FlexPDE at J_{sc}).The difference in the JV curves is so small that only the influence on the PV curves around mpp is represented in Fig. 8.

In general, the observed difference between the two PV curves obtained from lumped R_s and distributed R_s (FlexPDE computed) is very small. The difference is slightly higher for the 130 $\Omega/\square$ emitter than for the 77 $\Omega/\square$, as expected. It is interesting to note that the maximum power is slightly higher if one considers the lumped resistance calculation in comparison to the distributed one. This fact is surprising at the first glance

because the lumped resistance at mpp is lower than at J_{sc} and therefore a lower R_s at mpp should result, in a first intention, in a higher efficiency for the FlexPDE curve.
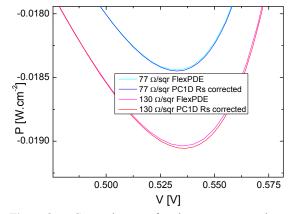

Figure 8: Comparison of the power voltage characteristics of the 77 Ω/□ and the 130 Ω/□ emitter solar cell as computed by FlexPDE and as calculated from the PC1D JV curves with the lumped R_s correction.

In Fig. 1b one can observe the level for which J_{source} reaches its average value J_{avg} at mpp. This current density value is therefore the one that would flow in a two-diode model circuit at mpp. It also corresponds to a certain bias voltage on the JV curve of the 130 Ω/□ emitter shown in Fig. 4 that is precisely at the same location in the voltage drop mapping (black line in Fig. 1a).

Representing also in Fig. 1a the potential drop induced by the series resistances when the cell delivers J_{avg} (grey level), one observes that these two levels do not superpose.

The grey level represents the voltage drop reached in a two-diode model lumped resistance and the black one represents the voltage drop level in the distributed resistance case. As the grey level is smaller than the black one, this demonstrates why the efficiency in the lumped resistance case is higher.

Then a difference of approximately 1 mV is observed between these two levels which multiplied by J_{avg} would lead to an efficiency difference of 0.03% for the 130 Ω/□ emitter which is what is observed in Fig. 8.

This maximum power differences should, however, not play a big role, particularly when considering that the measurement error is of this order.

This discrepancy is even smaller for the 77 Ω/□ emitter and therefore even more negligible.

4 STUDY OF A SELECTIVE EMITTER

Coming finally to the case of the selective emitter, we simulate a structure with the low R_{sh} emitter (77 Ω/□) until 100 μm from the finger and 150 μm from the busbar while the inner part of the emitter is the high R_{sh} emitter (130 Ω/□). In Fig. 9b the difference of source current density between the low and high R_{sh} emitter can be observed.

One can also observe in Fig. 9c that losses in the region close to the finger/busbar are lower because of the lower sheet resistance.

Besides the obvious practical advantage to contact more easily a low sheet resistance area, the compromise between a lower power loss close to the finger/busbar and the decrease of J_{source} in this region should be also considered for the optimal selective emitter, even if secondary.
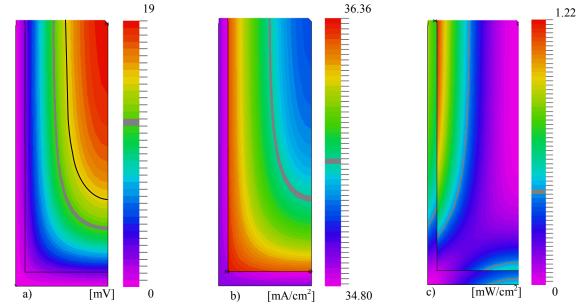

Figure 9: Distribution of a) the potential drop, b) the current density source distribution, and c) the dissipated power density in the emitter at the busbar (left edge) and finger (bottom edge) corner for an inter-finger distance of 1.9 mm, an inter-busbar distance of 50 mm and a selective emitter with low/high sheet resistance of 77/130 Ω/□ (zoom on busbar/finger corner).The grey level indicates the average current density source value J_{avg} in b), the average power loss density in c), and with $R_s \cdot J_{avg}$ the potential drop of the lumped series resistance crossed by J_{avg}. The black line in a) indicates the location of the average current density of b) in the potential map of a).
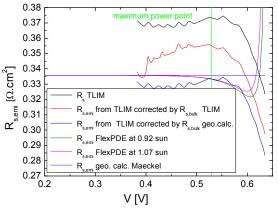
Figure 10: Comparison of $R_{s,emi}$ for: TLIM extracted values (black) corrected by $R_{s,bulk}$ obtained by TLIM (red) or calculated from the geometry (blue), $R_{s,emi}$ computed by FlexPDE at 0.92 and 1.07 sun illumination (dark green and pink curve, respectively), and $R_{s,emi}$ computed from the geometry by Wyeth's formula (purple) for the selective emitter.

This leads in general to an optimal extension of the low R_{sh} emitter of 100-150 µm after the finger/busbar. Luckily, these values usually correspond to the safety margins for alignment to ensure that the fingers/busbars are screen printed entirely in the low R_{sh} region.

One finally observe in Fig. 9a that the voltage drop map looks similar to the one of the high R_{sh} homogeneous emitter (see Fig. 1a), but the amplitude is slightly lower (maximum drops from 22 to 19 mV).

All these considerations lead to the fact that the series resistance should be significantly lower than in the homogeneous $130 \, \Omega/\square$ emitter case, as observed in Fig. 10.

A very troubling result of Fig. 10 is the fact that the FlexPDE curves are diverging to infinity when coming closer to V_{oc} while having a similar shape as for the homogeneous emitter on the rest of the $R_s(V)$ curve.

This is a consequence of the definition of the series resistance used in FlexPDE as we will see. Indeed V_{oc} condition implies that the total current density collected is zero.

In the case of the homogeneous emitter the Joule loss is also brought to zero and, strictly speaking, the series resistance is undetermined at this bias point.

However, in the case of the selective emitter the Joule losses are not brought to zero as a consequence of the different current density of the inner (low R_{sheet} emitter) and the outer cell (high R_{sheet} emitter).

Considering for the simplicity of the argumentation to discard the effect of the series resistance as well as the fact the inner cell does not have the same cell area as the outer cell, both cells can be considered in parallel and so having the same bias voltage.

As sketched in Fig. 11 there is one bias voltage for which the output current density is zero defining the V_{oc} of the solar cell. But this voltage point implies that the current density of the inner cell, which acts as a generator, is delivered entirely to the outer cell, which acts as a receptor.

While the total output current density is zero, this current density delivery from the outer to the inner cell through the emitter resistive layer induces a non-zero Joule loss.
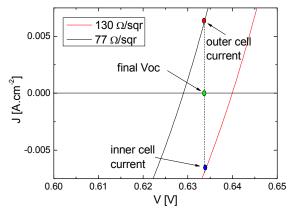

Figure 11: JV curves around V_{oc} obtained at 1 sun for the emitters of $R_{sheet}=77$ and $130 \, \Omega/\square$ without additional series resistance contribution.

Therefore, according to the definition of $R_{s,emi}$ of Eq. 3, one divides a non-zero Joule loss by a zero net output current squared, leading to an infinite value of $R_{s,emi}$ at V_{oc}.

This fact does not affect the computation of the simulated JV curve by FlexPDE and therefore the TLIM method can be performed without any issues.

Coming back to Fig. 10 the TLIM method does not produce such divergence of the curves close to V_{oc} which stay similar in shape to the one of the homogeneous emitter.

As explained in Sec. 2.2, the series resistance extracted from TLIM is defined as $\Delta V = R_s \cdot \Delta J$ where ΔJ is taken to be the difference in J_{sc} of curves at different illumination. Therefore ΔJ is never equal to zero, and there is no divergence of the $R_s(V)$ curve.

This discrepancy of the two methods around V_{oc} is therefore quite fundamental and raises the question of the overall validity of a realistic circuit based model in the case of the selective emitter at V_{oc} condition.

Taking into account the sheet resistance and the short circuit current density of high and low R_{sh} emitter as well as the global geometry of the selective emitter, Maeckel et al. [2] recently developed an analytical method that approximates very well the series resistance obtained by FlexPDE at J_{sc}. The geometrically calculated series resistance is in such case the one computed using the method of Maeckel et al. which is, like the method of Wyeth, voltage independent.

It is finally very interesting to observe in Fig. 10 that at mpp the TLIM corrected by the geometrically calculated bulk series resistance is almost perfectly matching the values derived by FlexPDE. The only hint to explain such fact comes from the fact that R_s was underestimated for low R_{sh} emitter (see Fig. 6) and overestimated for high R_{sh} emitter (see Fig. 7) by about the same amount. Therefore intuitively one might expect that the combination of both delivers a good approximation in the case of a selective emitter.

It is therefore particularly surprising that the most complicated structure, and therefore the one where the usual approximations of lumped series resistance, uniform source current density distribution and uniform diode model applies the least, delivers the best agreement between simulated and 'experimentally measured' series resistance.

There is presently no fully satisfactory explanation for this fact.

The disagreement between geometrically calculated series resistance and the two aforementioned values is also pretty low (less than 0.005 Ωcm^2).

5 DISCUSSION

It has been shown that all methods compared in this article conclude that the series resistance should reduce while going toward V_{oc} because of the non homogeneous current density source distribution. However, the R_s reduction observed at mpp is still low and its influence on the JV curve leads to a negligible discrepancy in efficiency even for a high sheet resistance emitter.

The finite element simulation of the $R_{s,emi}(V)$ curve, using as distributed current density source the JV curves of a one-dimensional cell simulated discarding series resistance, is considered the most realistic method in this study. Nevertheless, it leads to an unrealistic $R_{s,emi}(V)$ curve at V_{oc} condition of the selective emitter for a fundamental definition issue, while almost perfectly agreeing with the other simulations around mpp.

From this point of view it is not clear what should be modified in this simulation to make the various $R_{s,emi}$ determinations match at V_{oc}.

We suspect that the full physical simulation of this problem (by e.g. Synopsis Sentaurus), which would be an even more realistic simulation of this problem, would not bring more clarifications about this issue. This is because diffusion is also included and the Joule losses induced by drift are not easily separable from the ones induced by diffusion. In the definition of the series resistance, one however does not make the distinction between drift and diffusion in the origin of Joule loss, and therefore, strictly speaking, the methods investigated in this article would be invalid as they all assume only drift as an origin for Joule losses.

6 CONCLUSION

It has been shown in this contribution that the determinations of the series resistance contribution of the emitter from 'experimentally measured' JV curves, from analytical formula taking into account the emitter geometry, and from finite element simulation of Joule effects in the emitter agree well for all investigated situations at the maximum power point.

It is still not very clear why the agreement is so good, considering all the various kind of assumptions that are not strictly met for the various methods.

It is supposed that the various assumptions lead to discrepancies that are in any case small at mpp and sometimes even compensate each other, nearly regardless of the emitter structure.

This article, however, does not treat the case of non-uniform sheet resistance due to non uniform emitter formation and/or bulk non uniformity. In such case, however, one might think that the probable additional discrepancies would remain small. In any case the effect of considering the series resistance lumped or distributed in such case should have a smaller impact on the equivalent circuit modeling compared to the impact that such non uniformity in terms of lifetime in the bulk, emitter degradation and, probably above all, shunt due to

low parallel resistance would have.

It should be stressed that in the case of a cell concept where the relative contribution of the bulk series resistance to the total series resistance is significant (local back contacts, IBC, PERC …) an estimation of R_s by TLIM is always possible but is probably significantly different from drift based simulations or analytical formulas based on geometry because of the diffusion in the bulk.

7 REFERENCES

[1] FlexPDE 6.2, PDE Solutions Inc, 9408 E. Holman Rd., Spokane Valley, WA 99206, USA. http://www.pdesolutions.com

[2] H. Maeckel, G. Micard, K. Varner, Progr. Photovolt.: Res. Appl. 2013, in press, DOI: 10.1002/pip.2403.

[3] M. Wolf, H. Rauschenbach, Adv. Energy Conv. 3 (1963) 455.

[4] L.D Swanson, private communication with M. Wolf and H. Rauschenbach (see [3])

[5] N.C. Wyeth, Solid-State Electronics 20 (1977) 629.

[6] D.A. Clugston, P.A. Basore, Proc. 26th IEEE PVSC, (1997) 207.

[7] H. Haverkamp, A. Dastgheib-Shirazi, B. Raabe, F. Book, G. Hahn, Proc. 33rd IEEE PVSC (2009) 430.

[8] A. Goetzberger, B. Voss, J. Knobloch, Sonnenenergie Photovoltaik, Teubner, (1997)

[9] R. Brendel, S. Dreissigacker, N.-P. Harder, P.P. Altermatt, Appl. Phys. Lett. 93 (2008) 173503.